SECONDARY FLOW DEVELOPMENT IN A CASCADE LIKE PASSAGE OF A TURBOMACHINE.

AMER NORDIN DARUS
Fakulti Kejuruteraan Jentera, UTM

RINGKASAN

Makalah ini memaparkan formulasi analitik dan penyelesaian numerik aliran dimensi tiga yang rotasional di dalam sebuah saluran yang melengkung. Formulasi ini berdasarkan perhitungan halaju aliran dan komponen vortisiti selari axis saluran tersebut. Halaju sekunder ditentukan melalui penyelesaian serentak persamaan-persamaan keterusan dan vortisiti melalui penggunaan fungsi seperti fungsi arus. Hasil-hasil numerik diberikan dan dibandingkan dengan data-data eksperimen yang ada.

ABSTRACT

This article presents the analytical formulation and numerical solution of the three – dimensional rotational flow in curved duct. The formulation is based on calculating the flow – wise velocity and vorticity components from the momentum equation. The secondary velocities are determined from the simultaneous solution of the continuity and vorticity equations through the use of a streamlike function. The results presented are compared with the existing experimental data.

Secondary flow is a principle phenomena associated with the three dimensional flow in turbomachine compressors and turbines. It is defined here as the difference between the actual flow, and the flow which would occur on a two-dimensional axisymmetric and meriodional stream surfaces. Of the many factors that contribute to the development of secondary flow, end wall boundary layer is the most important. The interaction of the hub and casing slow moving boundary layer flow with the main flow, which is turning through the blades, results in the secondary flow. This interaction is caused by the blade to blade pressure gradient, the radial pressure gradient and the relative motion between the blade end. The annulus walls are additional factors that contribute to the establishment of the secondary flow.

In order to understand the physical nature of this secondary flow, let us consider what would happen to a flow with collateral boundary layer, or more generally a flow with a distorted velocity profile that enter a cascade. It is observed that secondary flow occurs in planes perpendicular to the curved passage's axis. There must be pressure gradient across the passage to balance the centrifugal force on the fluid due to its curved trajectory, the pressure being greater at the outer wall and smaller at the inner wall of the passage. The fluid near the top and bottom of the passage is moving more slowly than that near the central plane due to viscosity and therefore requires a smaller pressure gradient to balance its reduced centrifugal force. Consequently a secondary flow occurs in which the fluid near the top and bottom walls of the passage moves inwards towards the centre of the curvature of the central axis and the fluid near the central plane moves outwards. This in turn modifies the axial velocity. This phenomena was proved numerically by Austin (1) and Rushmore (2).

It is well known in turbomachinery (3) that secondary flow has an adverse effect on performance. A detailed review on this subject is given by Horlock and Lakshminarayana (4). A thorough understanding of this flow problem is therefore necessary to improve the performance of such turbomachines. Since a complete analysis of the problem in an actual machine is extremely difficult, see figure 1, various simpler models have been used. The flow in a curved rectangular channel has been frequently used for studying the secondary flow due to the streamline curvature. A comparison of the flow fields in bent passages and cascades is given in (5). It was observed that the streamlines are similar in a 60 degrees bend and a 60 degrees turning angle cascade, but the boundary layer flows are noticeably different in the two cases. This model has been successfully used by Fagan (6), Stuart and Hetherington (7), Hosney (8) and Abdallah (9). Rushmore (2) in his work, discussed in great details all the fluid models that he used in his study of curved 'duct flows'. The pertinence, applicability and shortcomings of these models were also pointed out.

MATHEMATICAL FORMULATION

The inviscid secondary flow theory was first devised by Squire and Winters (10), who demonstrated that if rectiliner shear flow with nonuniform velocity distribution enters a bend then secondary flow results. Their analysis is only valid for small turning angle. Hawthorne (11) using more complex vector manipulations generalised this result for larger turning angles. Marris (12), Lakshminarayana and Horlock (13) extended Hawthorne's analysis, giving a general vorticity equation valid for compressible, stratified and viscous flow.

In light of the previous work in this area, the governing equations are derived from the basic equations of conservation of mass and momentum for steady, inviscid and incompressible flow. The equations are written in cyclindrical polar co-ordinates to match the passage geometry, see figure (2), used in this study.

The momentum equations:

$$v\left(\frac{\partial v}{\partial r} + \frac{v}{r} - \frac{\partial u}{\partial \theta}\right) - w\xi = \frac{\partial p}{\partial r} \qquad (1$$

$$w\left(\frac{1}{r}\frac{\partial w}{\partial \theta} - \frac{\partial v}{\partial z}\right) - u\left(\frac{\partial v}{\partial r} + \frac{v}{r} + \frac{1}{r}\frac{\partial u}{\partial \theta}\right) = \frac{1}{r}\frac{\partial p}{\partial \theta} \qquad (2$$

$$u\xi - v\left(\frac{1}{r}\frac{\partial w}{\partial \theta} - \frac{\partial v}{\partial z}\right) = \frac{\partial p}{\partial z} \qquad (3$$

The Continuity equation:

$$\frac{\partial u}{\partial r} + \frac{u}{r} + \frac{I}{r}\frac{\partial v}{\partial r} + \frac{\partial w}{\partial z} = 0 \qquad (4$$

where (u, v, w) are the velocity components in the (r, 0 z) and the ξ component of the vorticity, respectively, defined as,

$$\xi = \frac{\partial u}{\partial z} - \frac{\partial w}{\partial r}$$

P is the total pressure divided by the density. The total pressure is eliminated from equations (1), (2) and (3) using crossed differentiation. The resulting equations which are solved for ξ and v are:

$$u\frac{\partial \xi}{\partial r} + \frac{v}{r}\frac{\partial \xi}{\partial \theta} + w\frac{\partial \xi}{\partial z} = \left(\frac{I}{r}\frac{\partial w}{\partial \theta} - \frac{\partial v}{\partial z}\right)\frac{\partial u}{\partial r}$$

$$+ \frac{\xi}{r}\frac{\partial v}{\partial \theta} + \left(\frac{\partial v}{\partial r} + \frac{v}{r} - \frac{I}{r}\frac{\partial u}{\partial \theta}\right)\frac{\partial v}{\partial z} \qquad (6$$

$$+ u\xi - v\left(\frac{I}{r}\frac{\partial w}{\partial \theta} - \frac{\partial v}{\partial z}\right) r$$

and,

$$u\frac{\partial v}{\partial r} + \frac{v}{r}\frac{\partial v}{\partial \theta} + w\frac{\partial v}{\partial z} = w\left(u\frac{\partial \xi}{\partial r} + \frac{v}{r}\frac{\partial \xi}{\partial \theta} + w\frac{\partial \xi}{\partial z}\right) + u\left(\frac{\partial v}{\partial r} - \frac{v}{r}\right)$$

$$- v\left(\frac{\partial u}{\partial r} - \frac{\partial w}{\partial z}\right)\left(\frac{\partial v}{\partial r} + \frac{v}{r} - \frac{I}{r}\frac{\partial u}{\partial \theta}\right) + w\xi\left(\frac{\partial u}{\partial r} + \frac{\partial w}{\partial z}\right)$$

$$+ w\left(\frac{I}{r}\frac{\partial w}{\partial \theta} - \frac{\partial v}{\partial z}\right)\left(\frac{v}{r} - \frac{\partial v}{\partial r}\right)\left(\frac{\partial v}{\partial r} + \frac{v}{r} - \frac{I}{r}\frac{\partial u}{\partial \theta}\right) \qquad (7$$

Full derivation of the above equations is straight forward but is very lengthy.
Initial and boundary conditions.

Refering to figure (2), the following initial and boundary conditions are used:

$$v(r, o, z) = v_1(z) \quad (8$$

$$\xi\,(r, o, z) = 0 \quad (9$$

$$u(Ri, 0, z) = O \quad (10a$$

$$u(Ro, 0, z) = 0 \quad (10b$$

$$w(r, 0, 0) = \quad (11a$$

$$w(r, 0, H) = 0 \quad (11b$$

Equations (1) to (7) with the boundary conditions (8) to (11) form a closed system which is solved for the variables u, ξ, v, w and

Computational Method of Solutions.

Equations (6) and (7), which represent a first order hyperbolic differential equation, can be written in the following general form: (12

$$u \frac{\partial f}{\partial r} + \frac{v}{r} \frac{\partial f}{\partial \theta} + w \cdot \frac{\partial f}{\partial z} = S$$

where f can be v or and S are the corresponding source term of equations (6) and (7) respectively. Referring to figure (3), let i,j,k refer to the indices of the grid point in the 0, r and z directions. Expressing the derivative with respect to 0 by first order accurate forward difference scheme, and the derivatives with respect to r and z by a second order accurate central differences scheme, equation (12) reduces to,

$$f_{i+1,j,k} = f_{i,j,k} + \left(\frac{ru}{\nu}\right)\left(\frac{\Delta\theta}{2\Delta r}\right)\left(f_{i,j+1,k} - f_{i,j-1,k}\right) + \left(\frac{r}{\nu}\right) S_{i,j,k} + \left(\frac{r\omega}{\nu}\right)\left(\frac{\Delta\theta}{2\Delta z}\right)\left(f_{i,j,k+1} - f_{i,j,k-1}\right) \quad (13)$$

Using Von Neumann method (14), this explicit finite difference expression for the values of the variables v and , at the grid point of (i + 1) plane, is unconditionally unstable. Thus to avoid this numerical unstability, a modification was made. It can be written as,

$$f_{i+1,j,k} = \frac{1}{4}\left[f_{i,j+1,k} + f_{i,j-1,k} + f_{i,j,k+1} + f_{i,j,k-1}\right] + \left(\frac{ru}{\nu}\right)\left(\frac{\Delta\theta}{2\Delta r}\right)\left(f_{i,j+1,k} - f_{i,j-1,k}\right) + \left(\frac{r}{\nu}\right) S_{i,j,k} + \left(\frac{r\omega}{\nu}\right)\left(\frac{\Delta\theta}{2\Delta r}\right)\left(f_{i,j,k+1} - f_{i,j,k-1}\right) \quad (14)$$

The condition of stability was found to be,

$$\frac{\Delta\theta}{\Delta r} \leq \frac{1}{r} \frac{v}{u}$$

This simple expression was based on the assumption, $u \simeq w$. Essentially, the hyperbolic equations (6) and (7) are solved using a marching technique.

The method of solving euqations (4) and (5) for the cross flow velocity components u and w will be briefly outlined here. More details about this technique can be found in (15). Equations (4) and (5) are first rewritten in the following forms:

$$\frac{\partial}{\partial r}(ru) + \frac{\partial}{\partial z}(rw) = -\frac{\partial v}{\partial \theta} \quad (15$$

and

$$\frac{\partial}{\partial z}(u) - \frac{\partial}{\partial r}(w) = \xi \quad (16$$

A new dependent variable, χ, is defined to satisfy the continuity equation (4) identically. The function χ is similar to the stream function, ψ, in satisfying the continuity equation identically, and is therefore called the streamlike function. The velocity components u and w are related to χ, through the following relations:

$$u = \frac{1}{r}\frac{\partial \chi}{\partial z} + \frac{1}{r}\int_{r_1}^{r}\left(-\frac{\partial v}{\partial \theta}\right) dr \quad (17$$

and

$$w = -\frac{1}{r}\frac{\partial \chi}{\partial r} \quad (18$$

where r_1 is a chosen reference value. The deviation from the standard definition of the stream function, ψ, , appears in the velocity component u, given by equation (17).

Then equations (17) and (18) are substituted into equation (16), one obtains:

$$\frac{\partial^2 \chi}{\partial r^2} - \frac{1}{r}\frac{\partial \chi}{\partial r} + \frac{\partial^2 \chi}{\partial z^2} = r\xi + \frac{\partial}{\partial z}\int_{r_1}^{r} \frac{\partial v}{\partial \theta}\, dr \quad (19$$

The boundary conditions, equations (10) and (11), are written in terms of the streamlike function χ as follows,

$$\frac{\partial \chi}{\partial z} = -\int_{r_1}^{r}\left(-\frac{\partial v}{\partial \theta}\right) dr \text{ at } r = Ri \text{ and } r = R_o \quad (20$$

and,

$$\frac{\partial \chi}{\partial r} = 0 \quad \text{at} \quad z = 0 \quad \text{and} \quad z = H \tag{21}$$

Integrating equations (20) and (21) along the boundaries, one obtains Dirichlet boundary conditions in terms of the streamlike function χ :

$$\chi = \int_{z_1}^{z} \int_{r_1}^{r} \frac{\partial v}{\partial \theta} \, dr\,dz + C_1 \quad \text{at } r = Ri \text{ and } r = R_o \tag{22}$$

and

$$\chi = C_2 \quad \text{at} \quad z = o \quad \text{and} \quad z = H \tag{23}$$

where C_1 and C_1 are constants to be evaluated from the continuity of the streamlike function at the corners of the rectangular cross section. Referring to figure 3, the finite difference representation for equation (20) using successive over relaxation is,

$$\chi_{i,j,k} = (1-\omega)\,\chi_{i,j,k} + \omega \Big[\alpha_1 \, \chi_{i,j+1,k} + \alpha_2 \, \chi_{i,j-1,k} + \beta(\chi_{i,j,k+1} + \chi_{i,j,k-1}) - \Delta z^2 S \Big] / 2\,(1+\beta) \tag{24}$$

where ω is the over-relaxation factor, and

$$\alpha_1 = \left(1 - \frac{\Delta r}{2r}\right) \beta \tag{25a}$$

$$\alpha_2 = \left(1 + \frac{\Delta r}{2r}\right) \beta \tag{25b}$$

$$\beta = (\Delta z / \Delta r)^2 \tag{26}$$

$$S = r\,\xi + \frac{\partial}{\partial z} \int_{r}^{r} \frac{\partial v}{\partial \theta} \, dr \tag{27}$$

Results and Discussion.

A computer program was developed to solve the equations governing the flow motion using the procedure outlined in the formulation and method of solution. The analysis was applied to the flow in the simple duct geometry of figure (2), whose cross section is a 5 x 5 inch square and whose mean radius is 15 inches. The flow resulting from a simple inlet velocity profile with linear variation in the z direction was investigated. The results are presented in a non-dimensional form, except the velocity contours. The duct inner radius R_i, and the maximum flow velocity at inlet V_{imax}, were used in the normalisation. The numerical computations were carried out in double precision on an AMDAHL 470 computer. The results presented here were generated using a (11 x 11 x 45) grid.

The results are presented in the form of velocity and secondary vorticity contours, and the vectors showing the magnitude and direction of the secondary velocities. The velocity contours at the 30°, 60° and 90° turning angles are shown in figures 5, 6 and 7. It can be seen from these figures that the rotation of the velocity, contours, which were parallel and horizontal at the inlet, is very significant in the first 60° of the duct. The contours become almost vertical before their rotation rate starts to decrease for turning angles greater than 60°

The secondary vorticity and the corresponding secondary velocities are shown in figures 8, 9 and 10 at 30°, 60° and 90° turning angles. A comparison of figures 8a, 9a and 10a reveals that the generated secondary vorticity reaches a maximum at the 30° cross section. It is interesting to recognise that with symmetric inlet velocity profile, the secondary vorticity is asymmetric and therefore vanishes at the plane of symmetry. It is also apparent from these figures that the vortex centre has moved towards the outer radius between the 30° and the 90° turning angles. The corresponding variations in secondary velocities can be seen in figures 8b, 9b and 10b. It is observed that, while the secondary velocities are comparable in magnitude at the 30° and 60° duct cross section they are significantly smaller at the 90° cross section. This is the region of very low secondary vorticity of figure 10a. In this region, all the velocity contours of figure 7, remain practically vertical with no appreciable rotation. It is interesting to see that the centre of rotation is different from the vortex centre in figures 8, 9 and 10. This difference can be attributed to the source term in the continuity equation which is caused by the variation in the through flow velocity component in the 0 – direction.

The available experimental results (16) in the lower half of Joy's duct are also presented for the purpose of qualitative comparison since the inlet profiles were not exactly the same as can be seen in figure (4). In spite of the differences between the inlet velocity profiles, it can be seen from figures (11) through (13) that the present analysis predicts not only the general trends reported in the experimental results, but also the magnitude of rotation of the constant velocity contours.

Acknowledgement

This research is supported by United States Air Force Office of Scientific Research Grant No. F 49620-78C-0041. This work is under the direction of Professor Awatef A. Hamed and supervised by Dr. Shaaban Abdallah, Department of Aerospace Engineering, University of Cincinnati, Ohio.

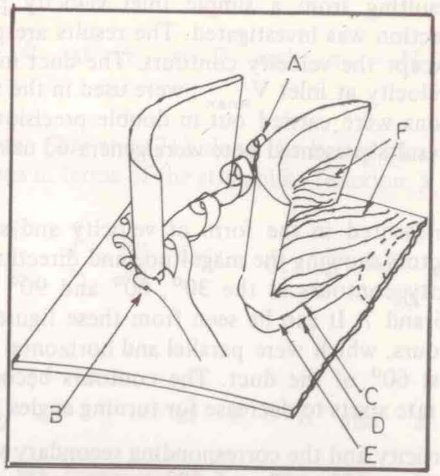

A Passage Vortex
B Horseshoe Vortex
C Separation Line of Passage Vortex
D Inlet Boundary Layer Separates
E Saddle Point
F Streamlines

Figure .1. Real Flow Phenomena in Cascade

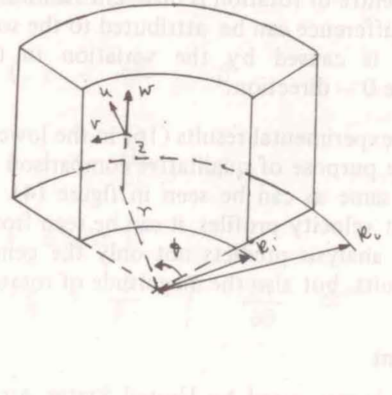

Figure. 2 Curved Duct Configuration

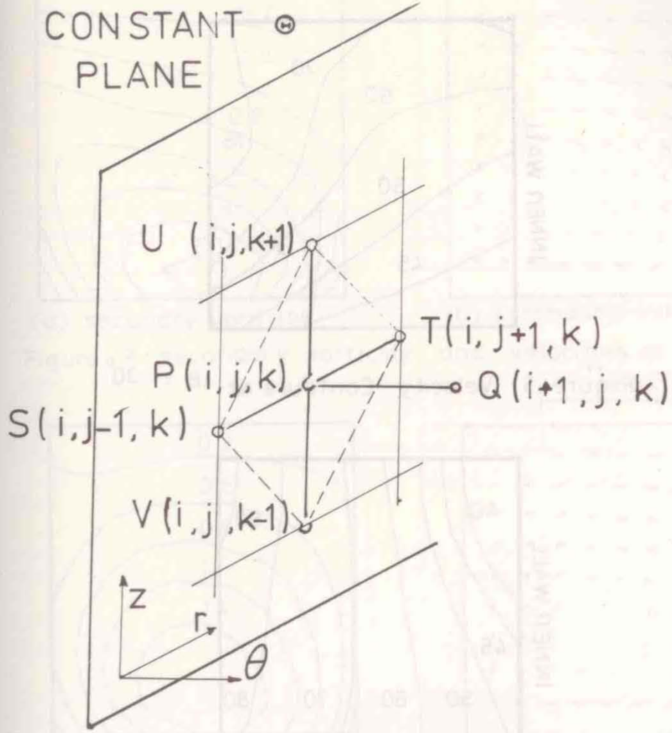

Figure. 3. Finite Difference Grid

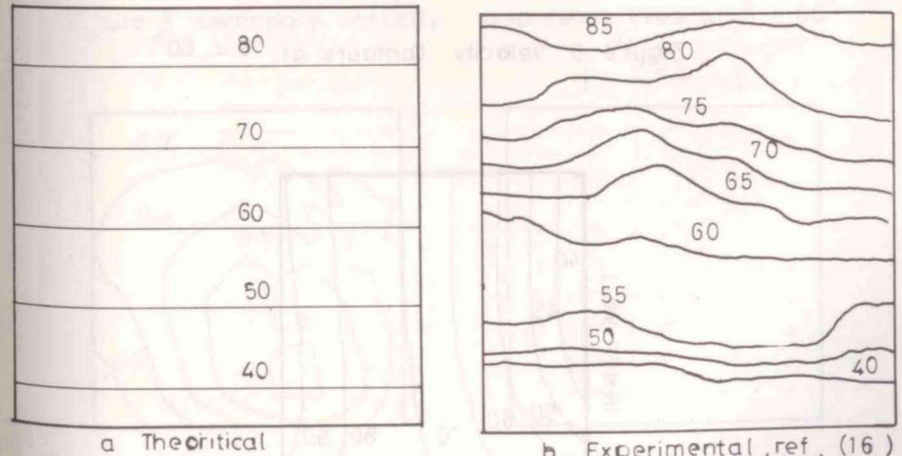

a Theoritical b. Experimental, ref. (16)

Figure 4 Inlet Velocity Profile

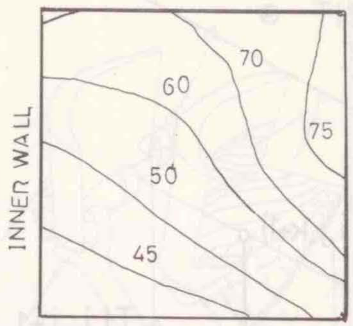

Figure 5. Velocity Contours at $\theta = 30^\circ$

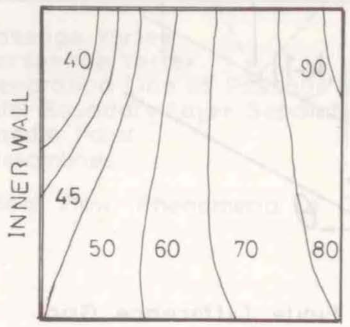

Figure 6. Velocity Contours at $\theta = 60^\circ$

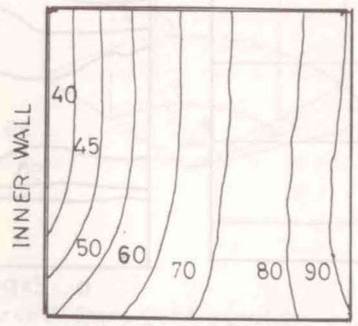

Figure. 7. Velocity Contours at $\theta = 90^\circ$

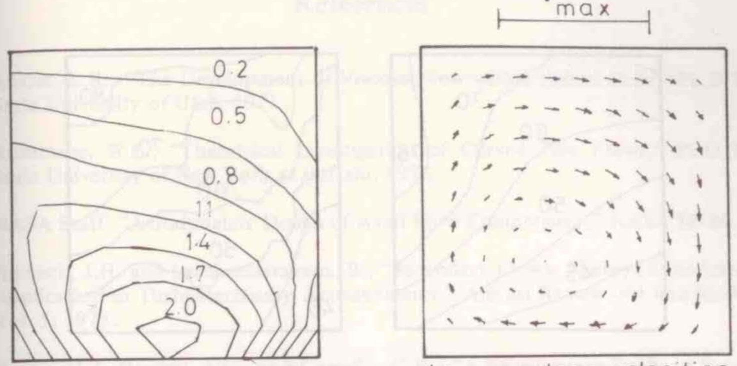

(a) secondry vorticity (b) secondary velocities

Figure 8 secondary vorticity and velocities at $\theta = 30^\circ$

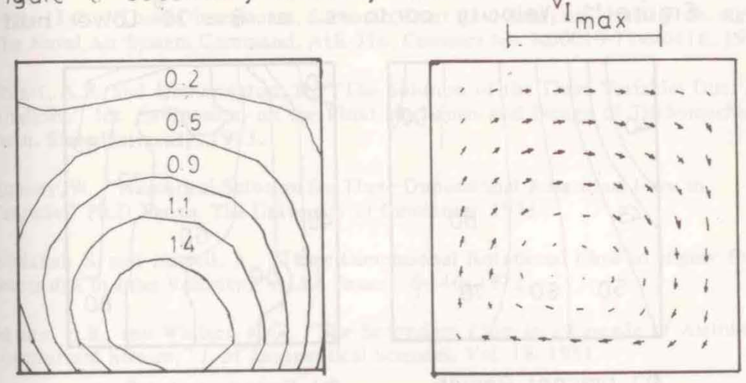

(a) secondary vorticity (b) secondary velocities

Figure 9 secondary vorticity and velocities at $\theta = 60^\circ$

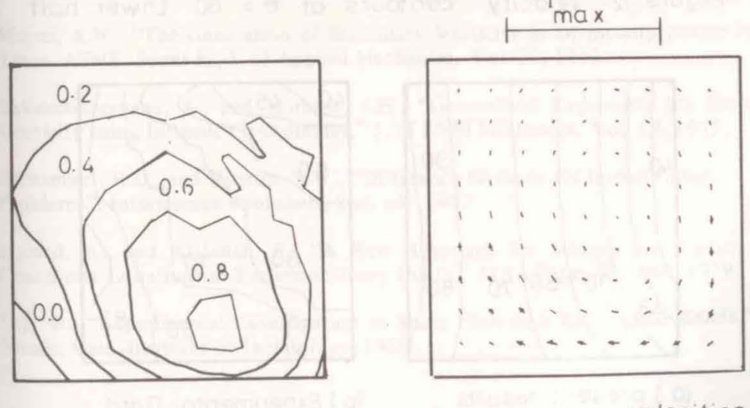

(a) secondary vorticity (b) secondary velocities

Figure 10 Secondary vorticity and velocity at $\theta = 90^\circ$

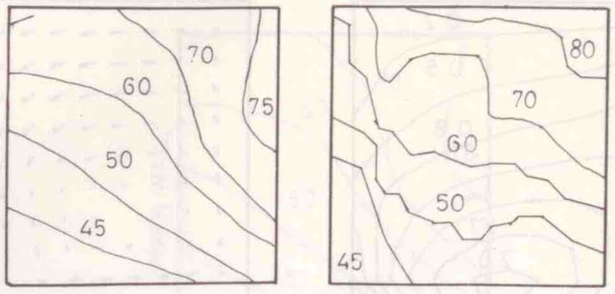

(a) present Result (b) Experimental Data Ref 15

Figure 11 Velocity contours at $\theta = 30^{\circ}$ Lower half

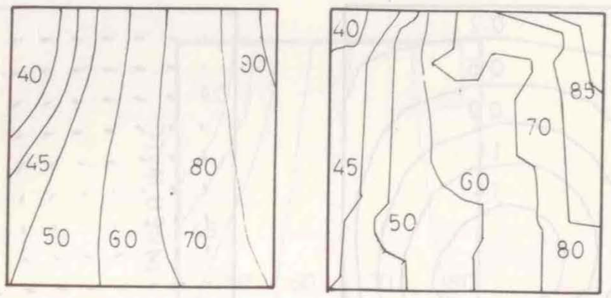

(a) present Result (b) Experimental Data Ref 15

Figure 12. Velocity contours at $\theta = 60^{\circ}$ Lower half

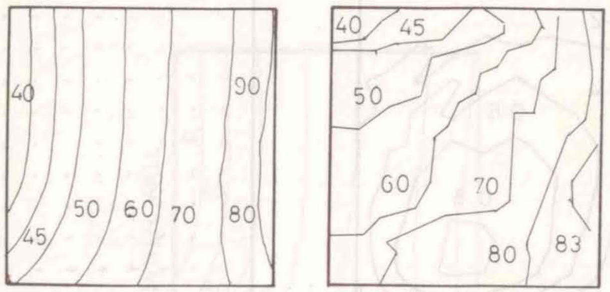

(a) present results (b) Experimental Data Ref (15)

Figure 13 Velocity contours at $0 = 90^{\circ}$ Lower half

References

1. Austin, L.R., "The Development of Viscous Flow within Helical Coils, "Ph.D Thesis, State University of Utah, 1971.

2. Rushmore, W.L., "Theoritical Investigation of Curved Pipe Flows," Ph.D Thesis, State University of New York at Buffalo, 1975.

3. NASA Staff, "Aerodynamic Design of Axial Flow Compressors," NASA SP-26, 1965.

4. Horlock, J.H. and Lakshminarayana, B., "Secondary Flows: Theory, Experiment and Application in Turbomachinery Aerodynamics," Annual Review of Fluid Mechanics, Vol. 5, 1975.

5. Herzig, H.Z. Hansen, A.G., and Costello, G.R., "A Visualisation Study of Secondary Flow in Cascades," NACA Rept. 1163, 1954.

6. Fagan, J.R., "Three-Dimensional, Subsonic, Duct flow Analysis," Final Tech. Report, The Naval Air System Command, AIR-310, Contract No. N00019-71-6-0416, 1973.

7. Stuart, A.R. and Hetherington, R., "The Solution of the Three Variables Duct Flow Analysis," Int. Symposium on the Fluid Mechanics and Design of Turbomachinery, Penn. State University, 1973.

8. Hosney, W., "Numerical Solution for Three-Dimensional Rotational Flow in Cascade," Ph.D Thesis, The University of Cincinnati, 1975.

9. Abdallah S. and Hamed, A., "Three-Dimensional Rotational Flow in Highly Curved Ducts due to Inlet Velocity," AIAA Paper -78-146, 1978.

10. Squire, H.B., and Winters, K.G., "The Secondary Flow in a Cascade of Airfoils in a nonuniform Stream," J. of Aeronautical Sciences, Vol. 18, 1951.

11. Hawthorne, W.R., "Secondary Circulation in Fluid Flow," Proceedings of the Royal Society, Vol. 206, 1951.

12. Marris, A.W., "The Generation of Secondary Vorticity in an Incompressible Fluid," Trans. ASME, Series E., J. of Applied Mechanics, Vol. 30, 1963.

13. Lakshminarayana, B., and Horlock, J.H., "Generalised Expression for Secondary Vorticity using Intrinsic Co-ordinates," J. of Fluid Mechanics, Vol. 59, 1973.

14. Richtmyer, R.D., and Morton, K.W., "Difference Methods for Initial-Value Problems", Interscience Publishers, 2nd. ed., 1967.

15. Hamed, A., and Abdallah, S., "A New Approach for Solving the Vorticity and Continuity Equations in Turbomachinery Ducts," AIAA Paper-79-0046, 1979.

16. Joy, W., "Experimental Envestigation of Shear Flow in a Rectangular Bends," M.Sc Thesis, Mass. Institute of Technology, 1950.